Supporting Information

Biological sealing and integration of fibrinogen-modified titanium alloy with soft and hard tissues in a rat model

Xiuli Wang[a, 1], Xing Lei[b,c, 1], Yue Yu[a], Sheng Miao[b], Jingyu Tang[a], Ye Fu[a], Kai Ye[a], Yang Shen[a], Jiayue Shi[a], Hao Wu[b], Yi Zhu[a], Lin Yu[a], Guoxian Pei[b,d], Long Bi[b, *], Jiandong Ding[a, *]

[a] State Key Laboratory of Molecular Engineering of Polymers, Department of Macromolecular Science, Fudan University, Shanghai 200438, China

[b] Department of Orthopedics, Xijing Hospital, The Fourth Military Medical University, Xi'an 710032, China

[c] Department of Orthopedic Surgery, Linyi People's Hospital, Linyi 276000, China

[d] Southern University of Science and Technology Hospital, Southern University of Science and Technology, Shenzhen 518055, China

[1] These two authors contributed equally.

* Corresponding authors. E-mail addresses: jdding1@fudan.edu.cn (J.D. Ding), bilong@fmmu.edu.cn (L. Bi)

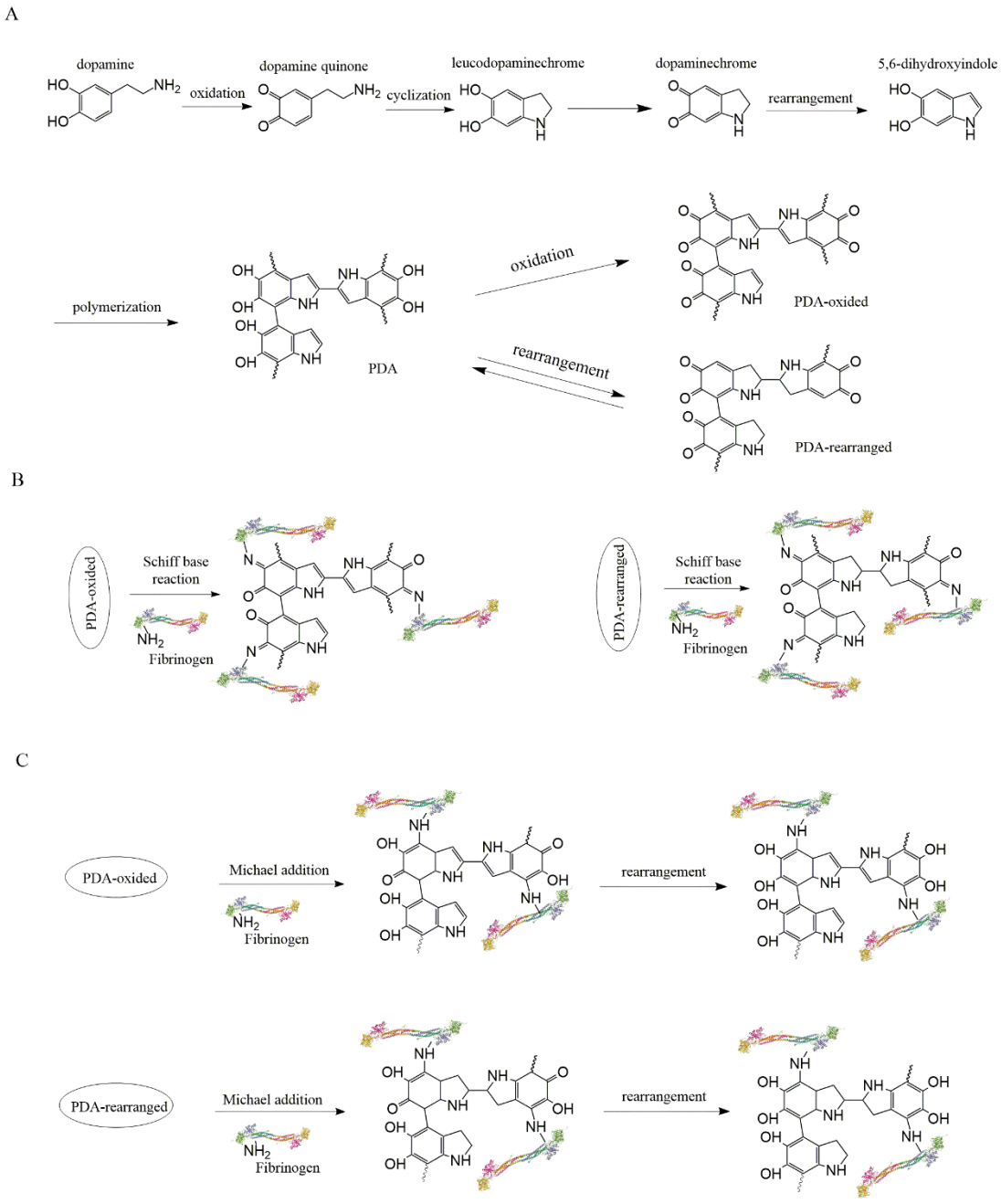

Figure S1 The formation process of polydopamine (PDA) and its interaction with fibrinogen. (A) The synthesis route of PDA and its oxidation/rearrangement products. The possible reaction mechanism between PDA-oxided/PDA-rearranged products and fibrinogen through Schiff base reaction (B) or Michael addition reaction (C).

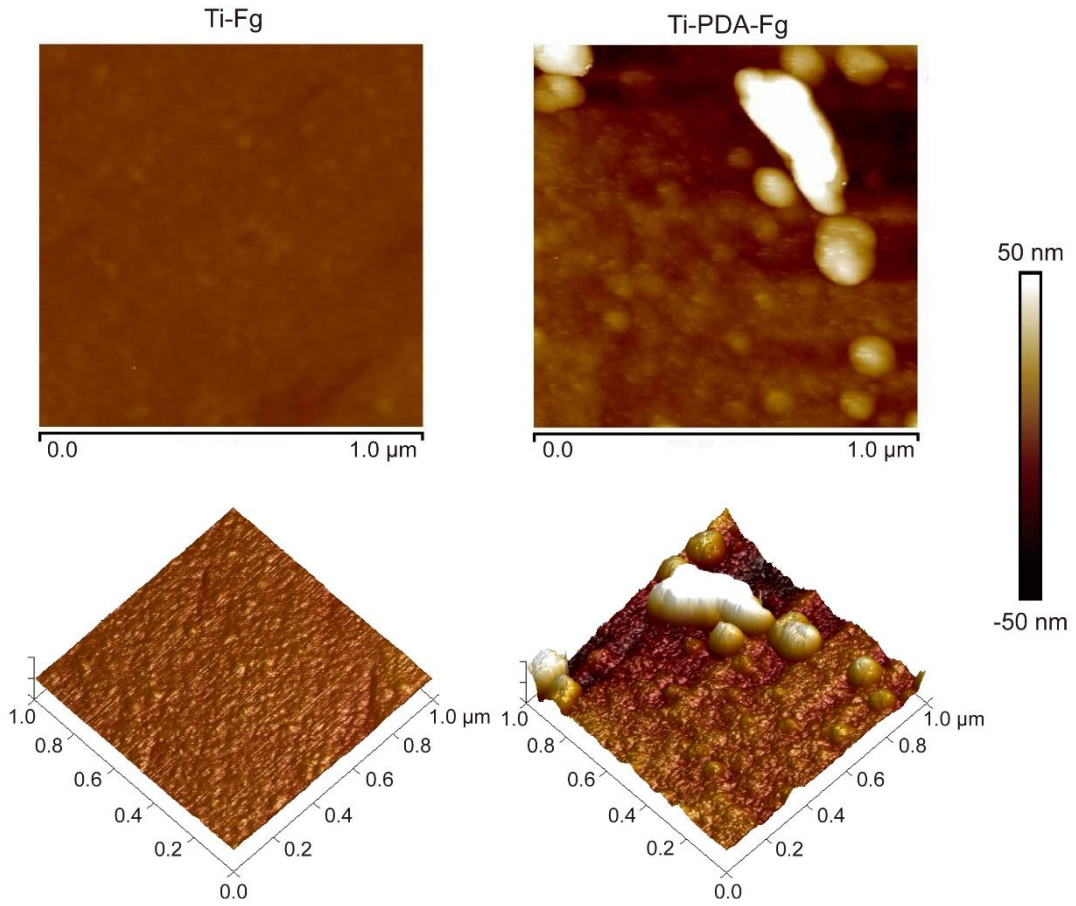

Figure S2 High-magnification AFM images of Ti-Fg and Ti-PDA-Fg.

Table S1 The atomic composition of the modified titanium surfaces characterized by XPS.

	C/%	N/%	O/%	Ti/%
Ti(control)	49.40	0.90	41.60	8.00
Ti-PDA	69.20	6.40	22.30	2.10
Ti-PDA-Fg	73.21	8.75	17.98	0.06
Ti-PDA-Fg 3 day	73.11	8.01	18.74	0.14
Ti-Fg	42.51	5.50	41.86	10.12
Ti-Fg 3 day	40.60	2.51	46.54	10.35

Note: Here “Ti” refers to Ti-6Al-4V titanium alloy. Such an abbreviation is for convenience to describe the four groups of alloy surfaces with and without the indicated modifications (Ti, Ti-Fg, Ti-PDA, Ti-PDA-Fg).

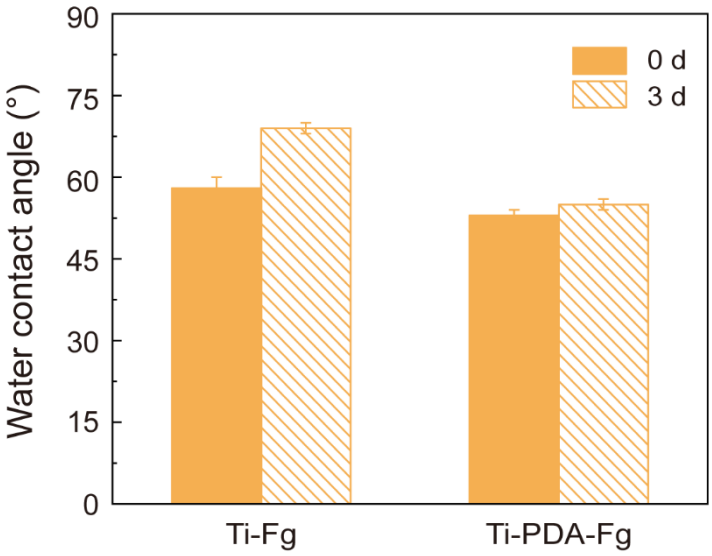

Figure S3 Static water contact angles of Ti-Fg and Ti-PDA-Fg surfaces before and after being immersed in phosphate buffer saline (PBS) solution placed in a water bath shaker for three days.

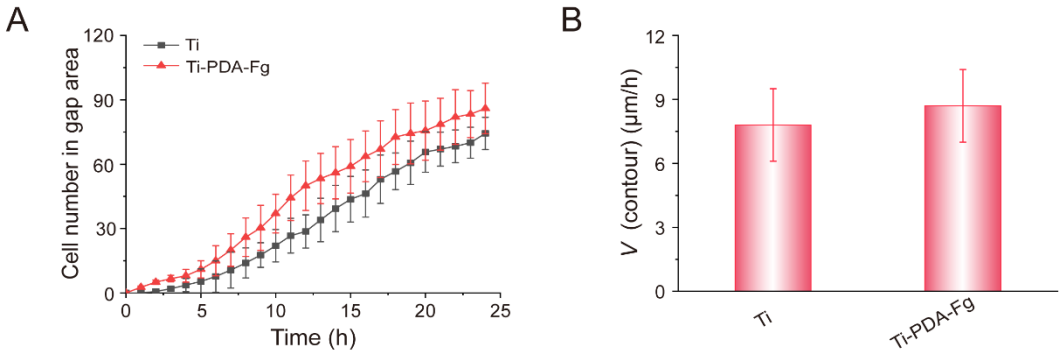

Figure S4 Numbers of fibroblasts (HFF) migrated into the gap areas in collective cell migration experiments at the indicated time points, and the calculated *V*(contour) in single-cell migration experiments.

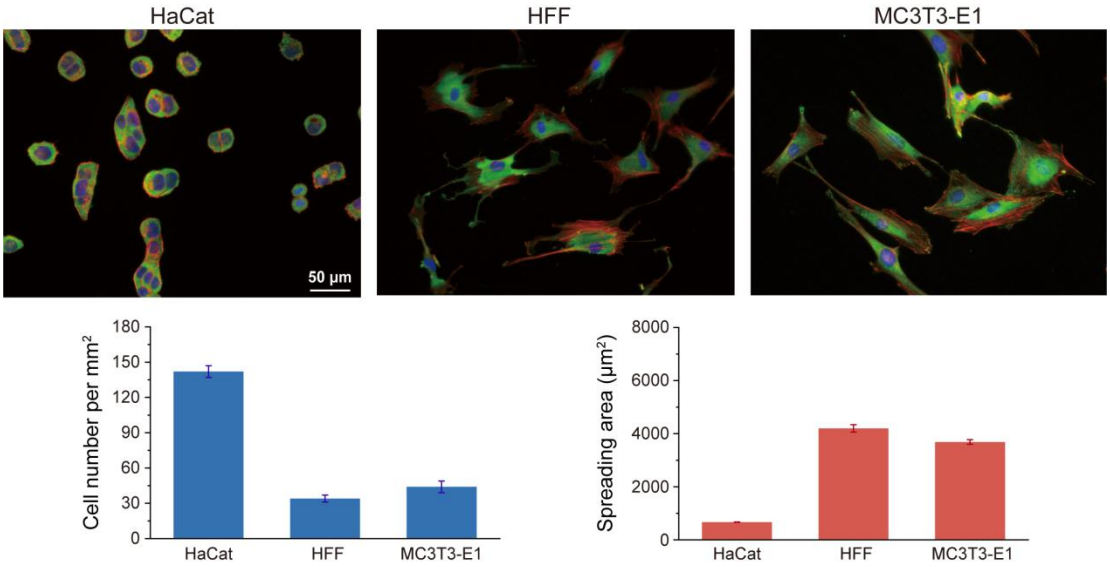

Figure S5 Keratinocytes (HaCaT), fibroblasts (HFF) and preosteoblasts (MC3T3-E1) on the Ti-PDA surfaces after 12 hours of culture, reflected by fluorescence micrographs of the stained cells with vinculin in green, F-actin in red, and nuclei in blue, and the corresponding statistic results of cell adhesion parameters.

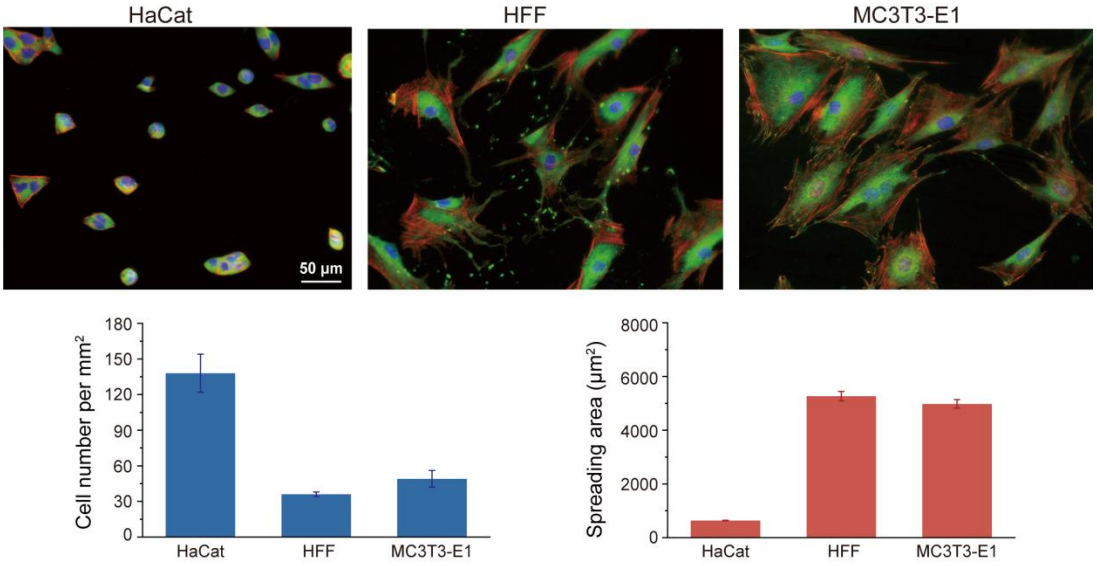

Figure S6 Similar to Fig. S5 except that the sample is Ti-Fg.

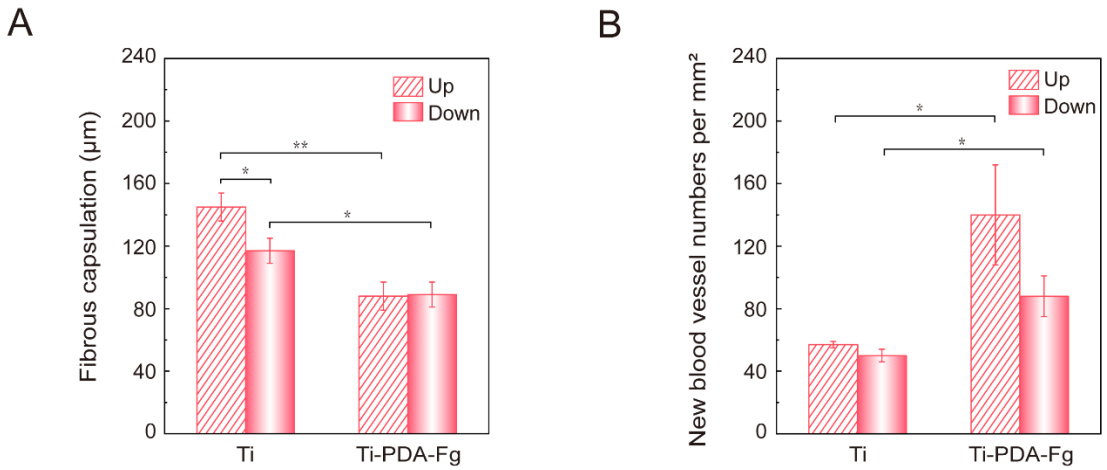

Figure S7 Statistical results of the thickness of fibrous capsulation (A) and the number of new blood vessels (B) from the indicated samples of metal sheets (n = 3) after subcutaneously implanted into SD rats.

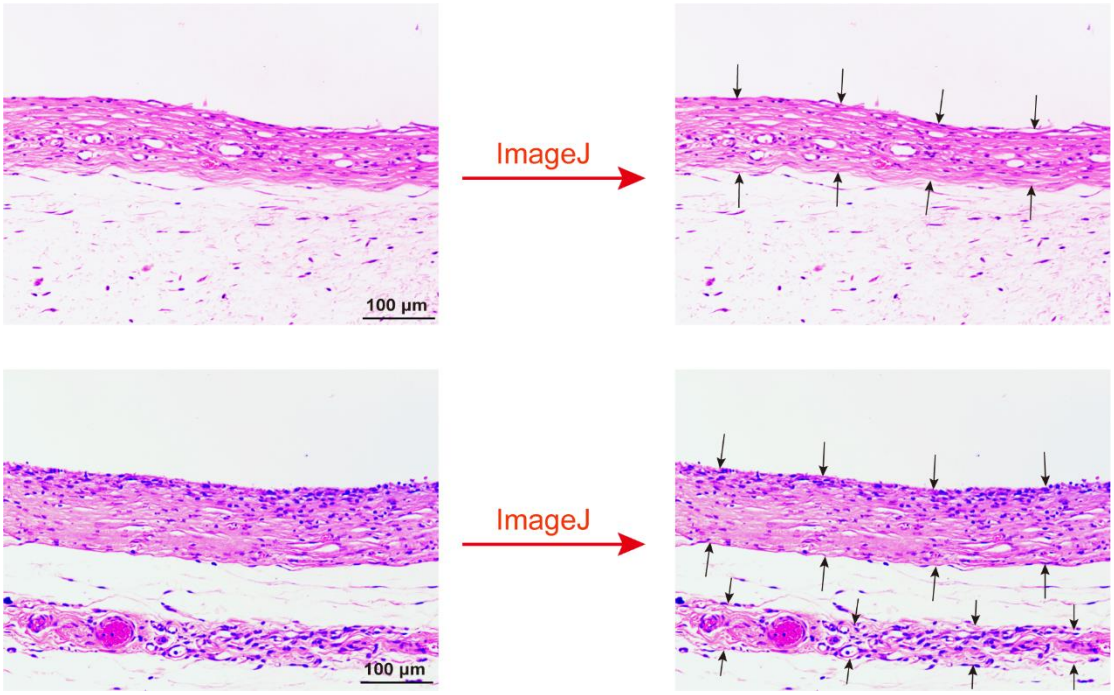

Figure S8 Optical micrographs of HE stained slices for calculation of the thickness of fibrous capsulation. Some positions of each stained images are indicated by the black arrows, and in some cases the thickness of the torn part of capsulation should also be included.

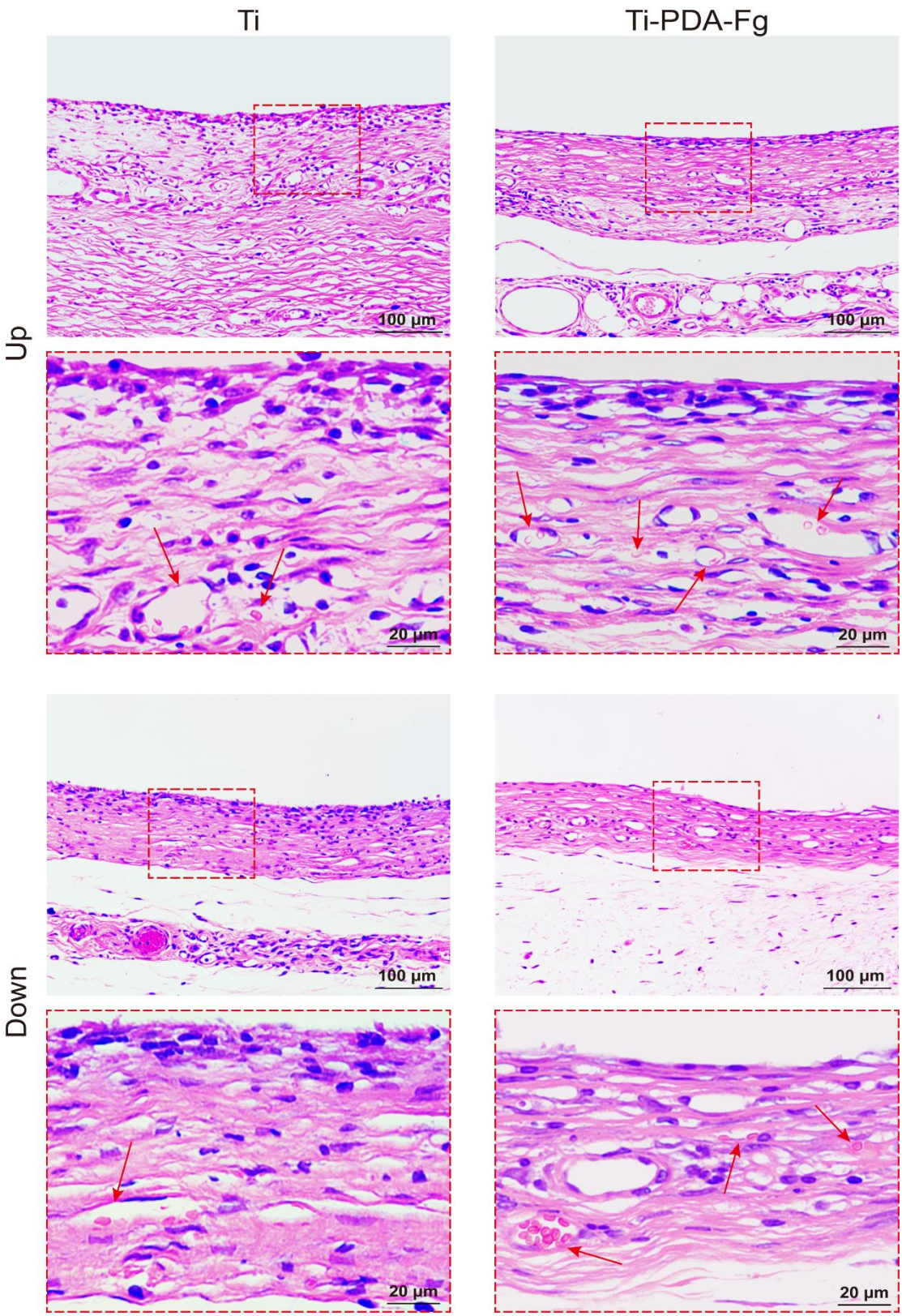

Figure S9 Optical micrographs for histological analysis of the biopsy of the capsule surrounding Ti and Ti-PDA-Fg sheets subcutaneously in SD rats. The specimens were HE stained prior to observations. The metal sheets were removed before slicing, and thus the blank area at the top of

the indicated picture represents the location of the metal sheet. The side facing the fibrous capsule is the ‘modified surface’. The lower images are magnified ones of the regions in the upper ones as marked by the dashed squares. The arrows indicate some blood vessels.

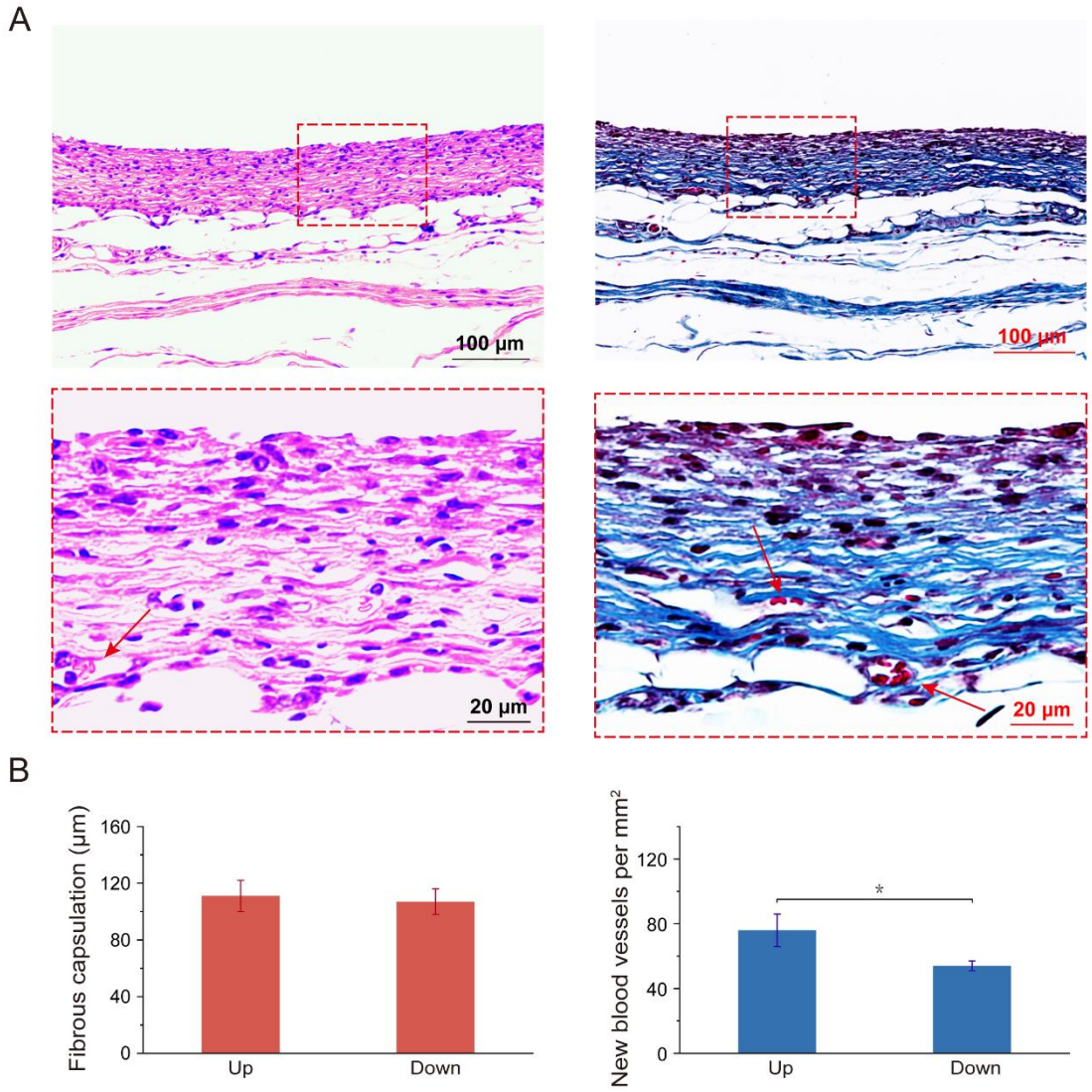

Figure S10 Histological analysis of the biopsy of the capsule surrounding Ti-PDA samples by HE staining and Masson’s trichrome staining (A) and corresponding statistical results (B). The blank area at the top of the indicated picture represents the location of the metal sheet, and the side facing the fibrous capsule is the ‘modified surface’. The metal sheets were removed before slicing.

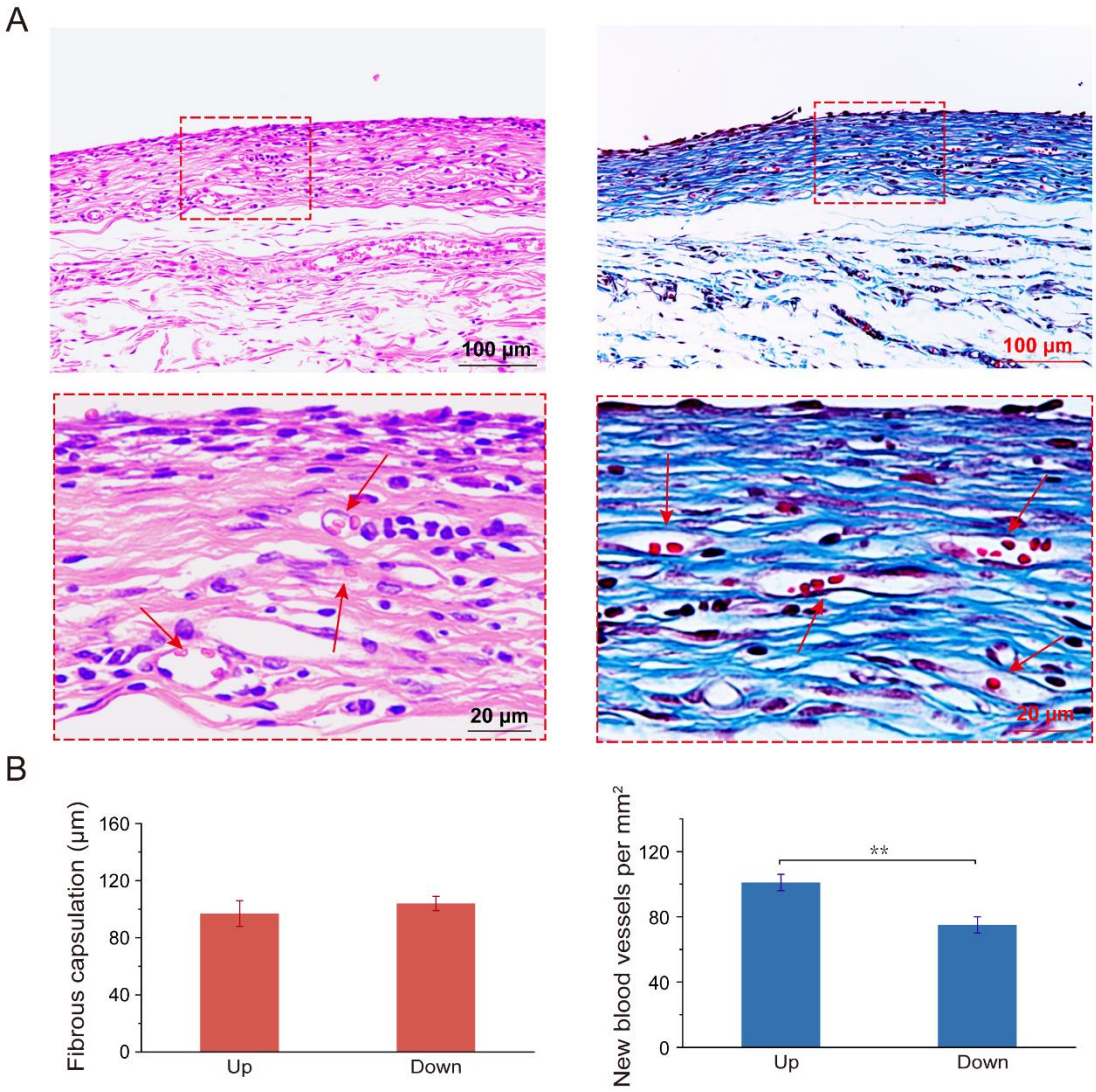

Figure S11 Similar to Fig. S10 except that the sheet sample is Ti-Fg.

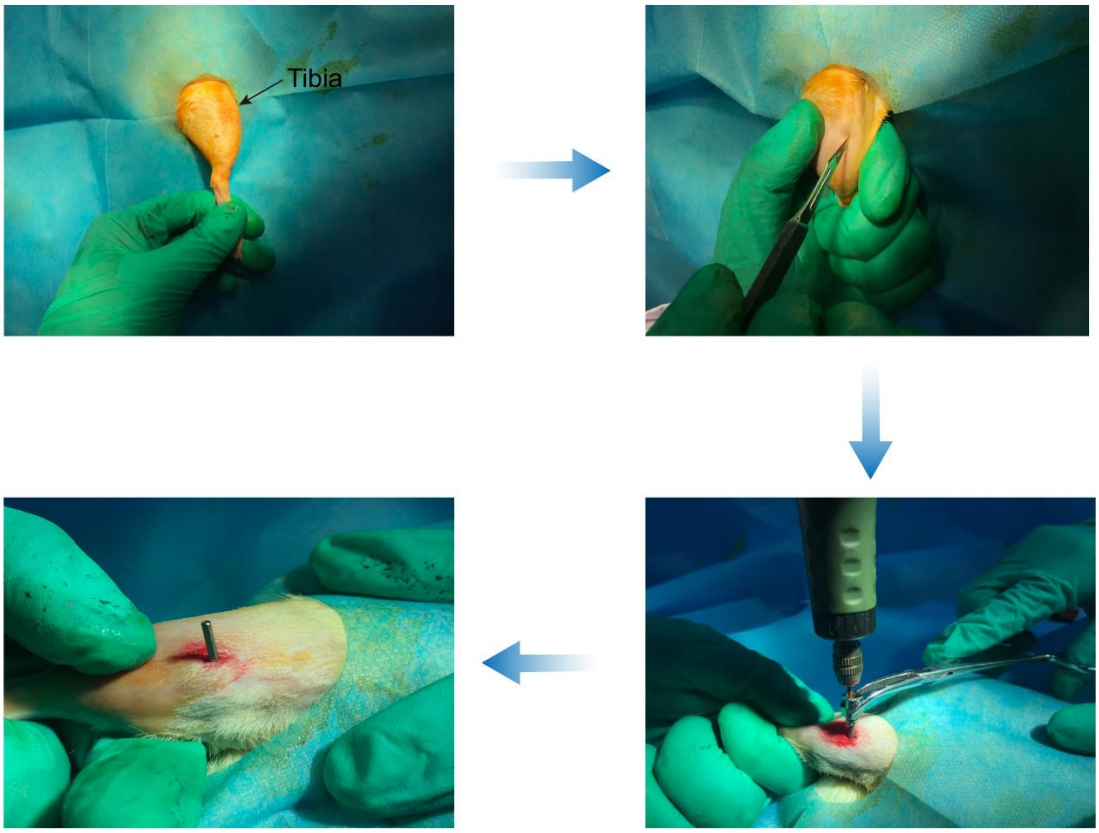

Figure S12 Global view to demonstrate the surgical implantation procedure of a metal screw into a leg of an SD rat.

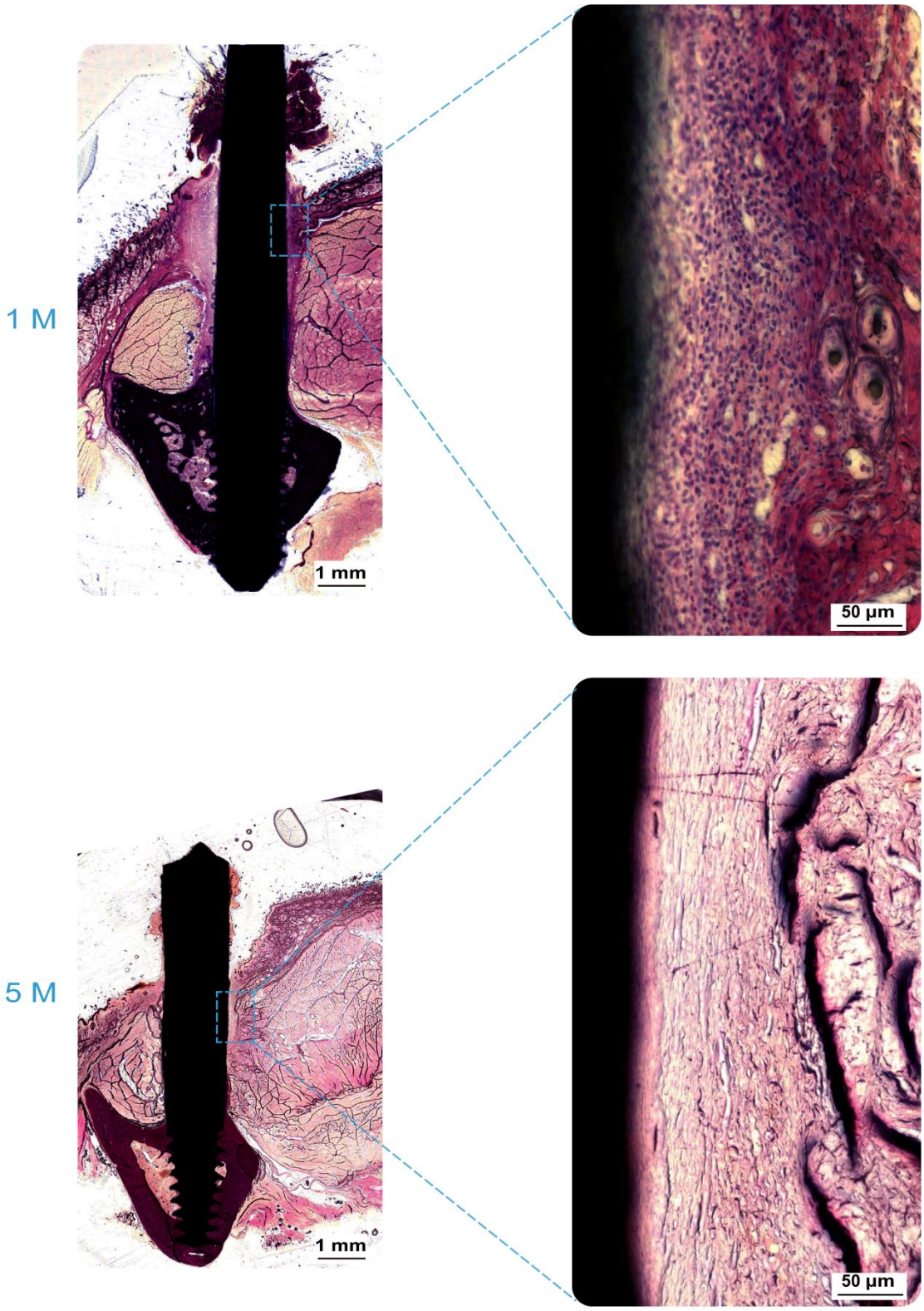

Figure S13 Histological images of HE-stained tissue sections of a Ti screw after implanted for 1 month and 5 months. A plenty of inflammatory cells with nuclei stained in dark blue were observed in the upper-right image.

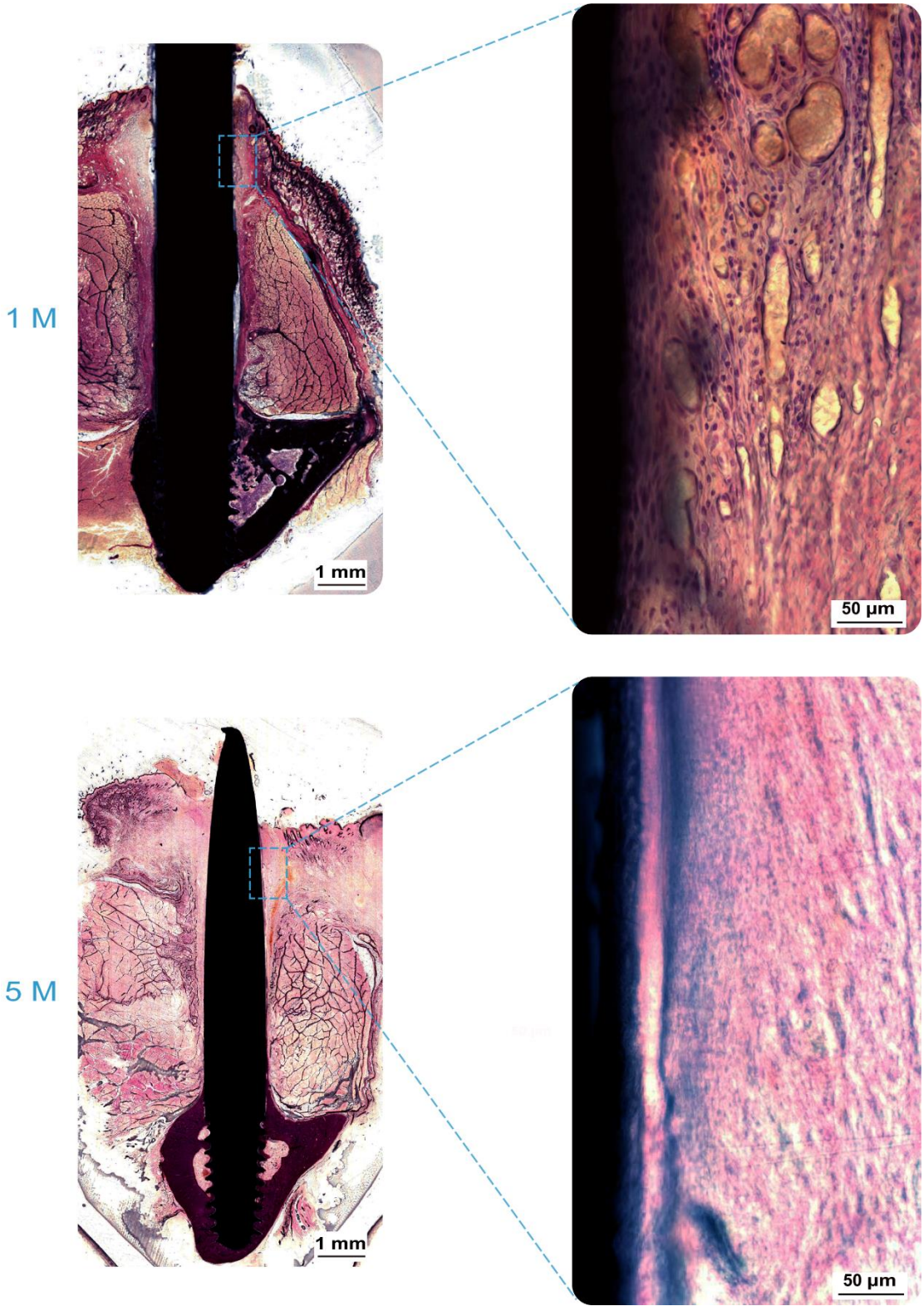

Figure S14 Similar to Fig. S13 except that the screw sample is Ti-PDA-Fg.

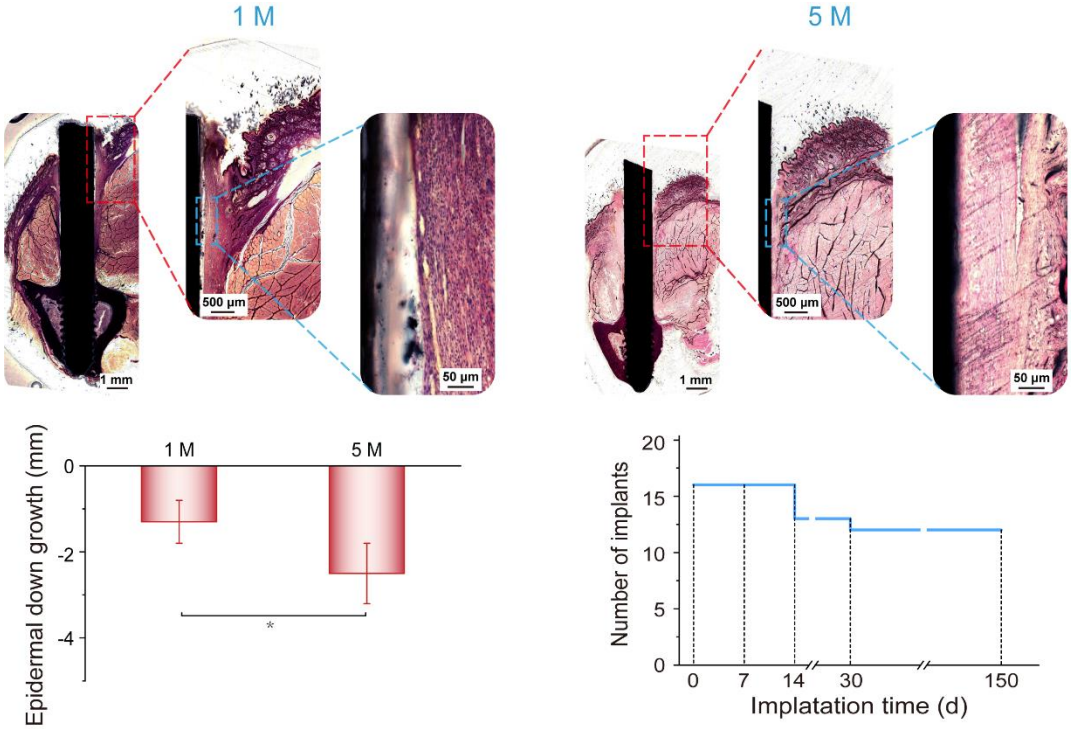

Figure S15 (up) Histological images of HE-stained tissue sections of Ti-PDA screw at 1 month and 5 months. (down) The distance of epidermal downgrowth was analyzed using ImageJ software (n = 4) and the number of implants during implantation time.

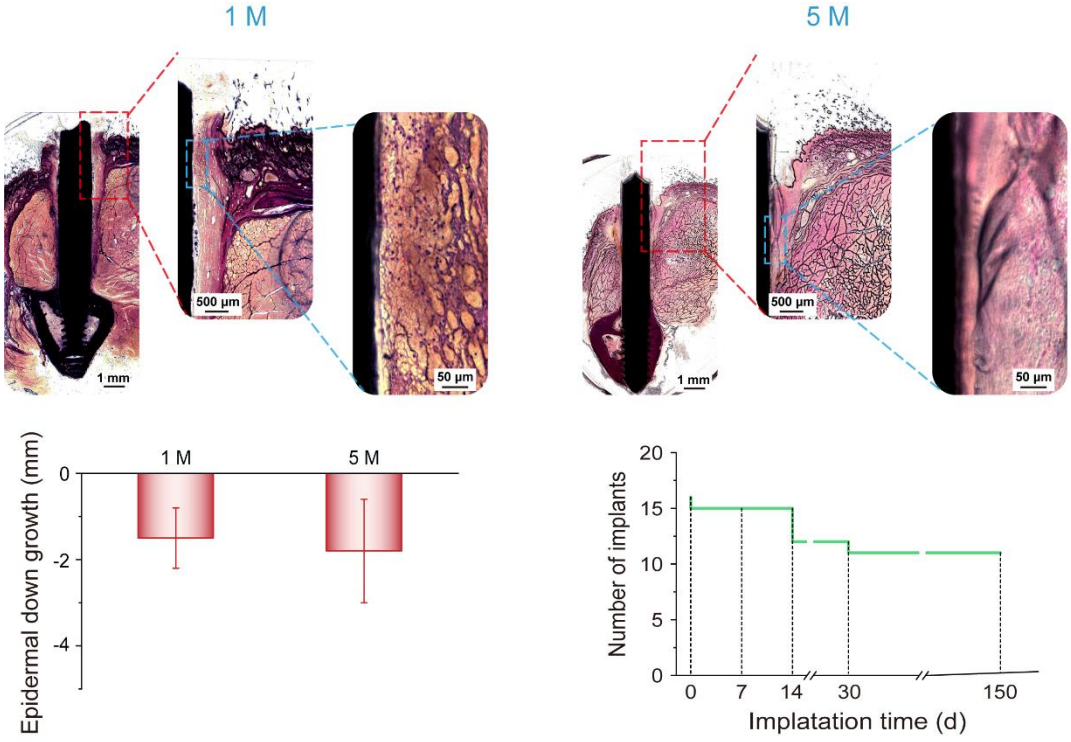

Figure S16 Similar to Fig. S15 except that the screw sample is Ti-Fg.

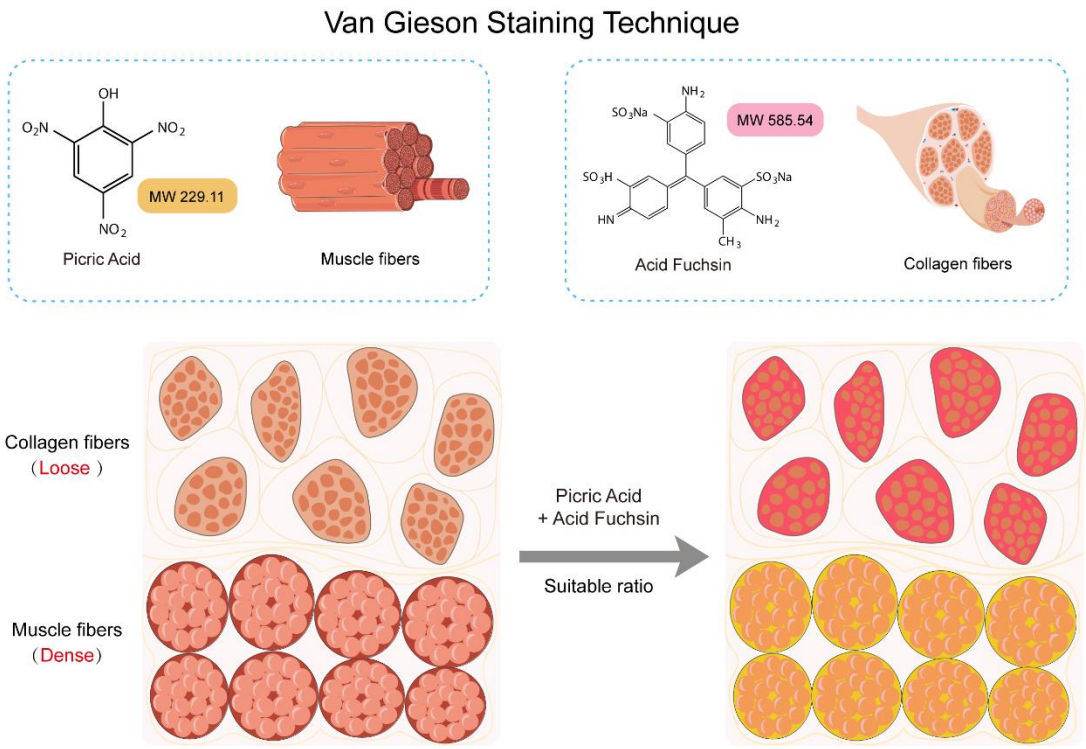

Figure S17 Schematic illustration of Van Gieson (VG) staining technique. The principle of VG staining is related to the size of anionic dye molecules and the permeability of tissues. Low molecular weight dyes can easily penetrate tissues, while dyes with high molecular weight can only enter tissues with loose structure and high permeability. In VG staining, muscle fibers are stained in yellow by picric acid, and collagen fibers are stained in red by acid fuchsin.

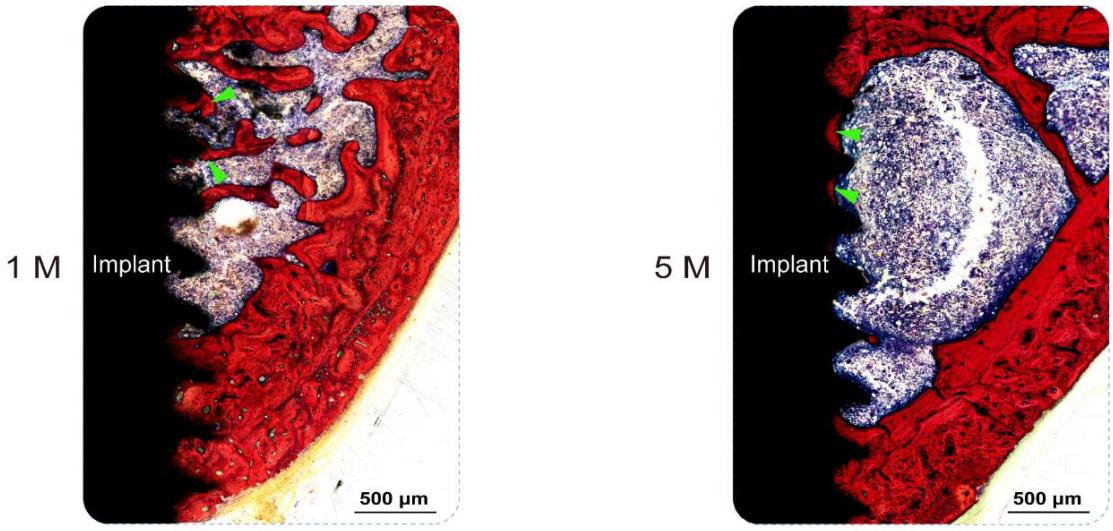

Figure S18 Histological images of VG-stained hard tissue sections of Ti implants at 1 month and 5 months. The new bone was stained red (as shown by the green arrow), and the fibrous tissue was stained blue.

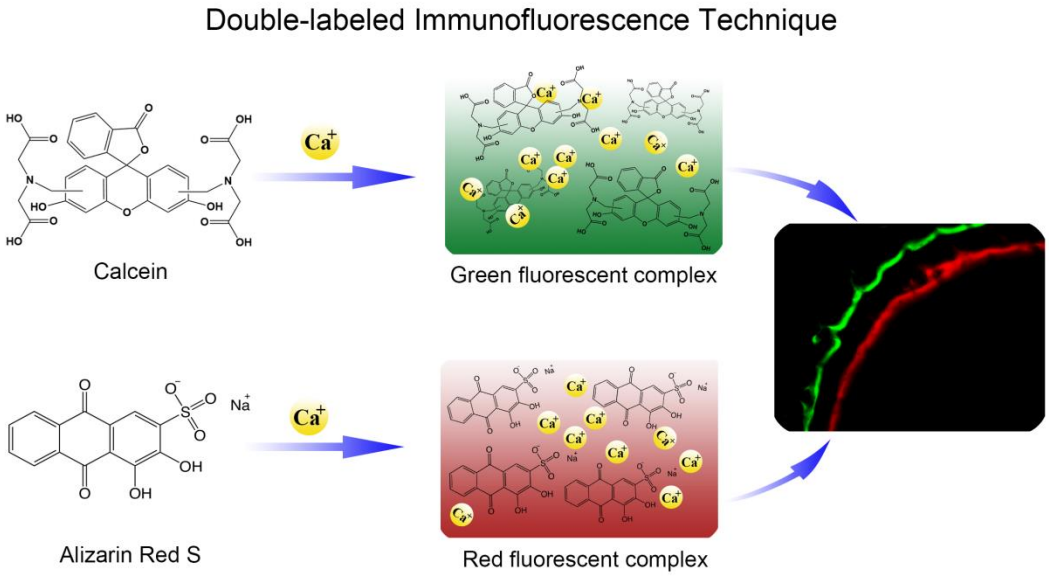

Figure S19 Schematic illustration of double-labeled immunofluorescence technique to visualize new bone generation frontiers at two different times. Calcein and alizarin red S can combine with calcium ions to generate green fluorescence and red fluorescence complexes, respectively.

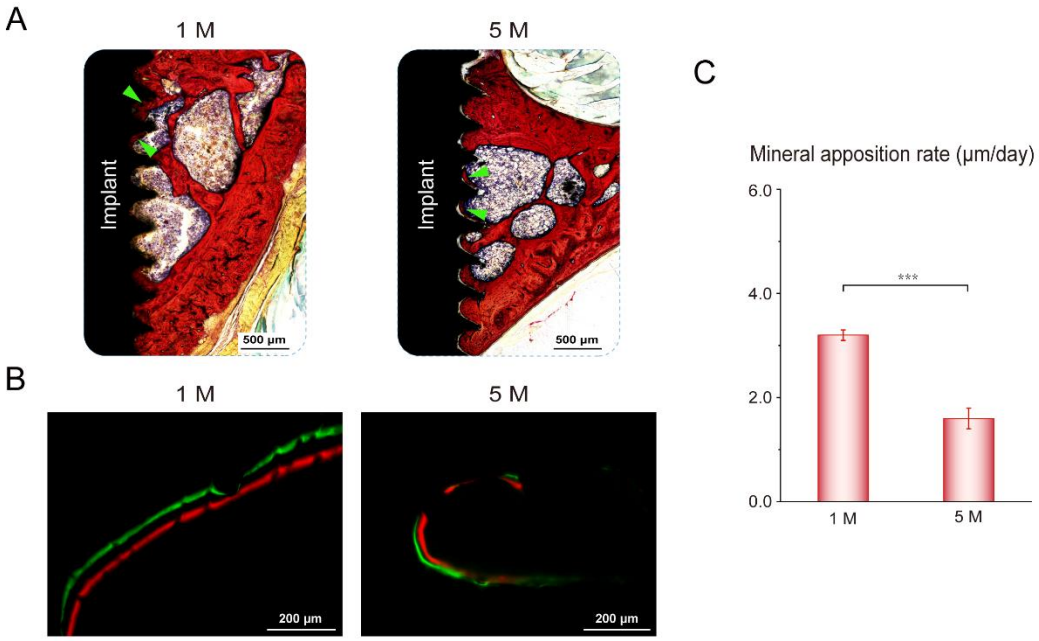

Figure S20 (A) Histological images of VG-stained hard tissue sections of Ti-PDA implants at 1 month and 5 months. The new bone was stained red (as shown by the green arrow), and the fibrous tissue was stained blue. (B) Double-labeling immunofluorescence images of the Ti-PDA group under a fluorescence microscope. After blue light irradiation, calcein showed green under microscopy, and alizarin red S showed red after red light irradiation. (C) Mineral apposition rate of bone (n = 4).

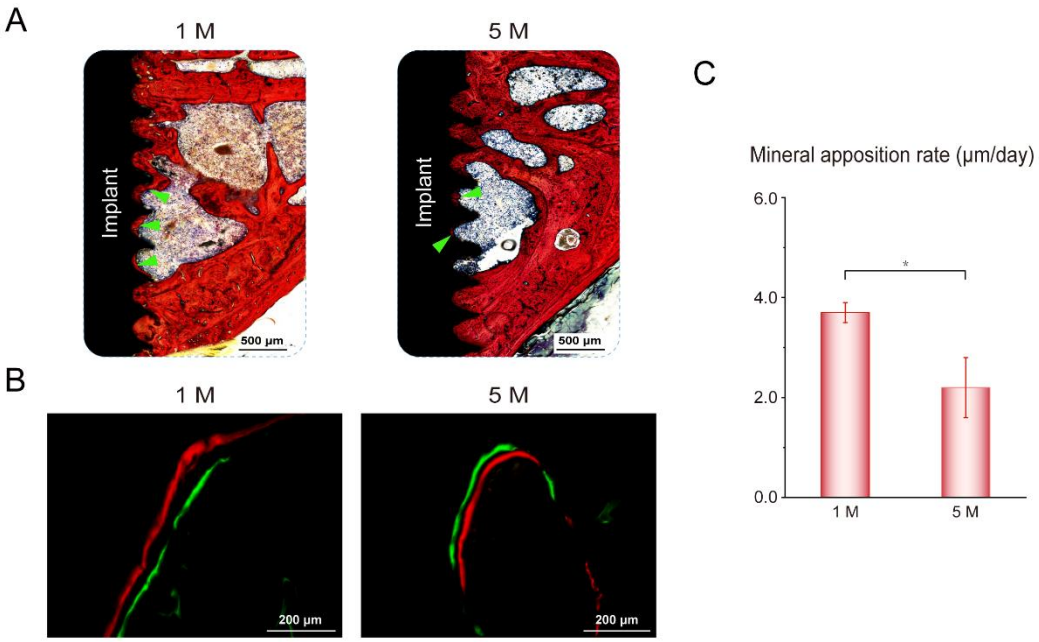

Figure S21 Similar to Fig. S20 except that the sample is Ti-Fg.

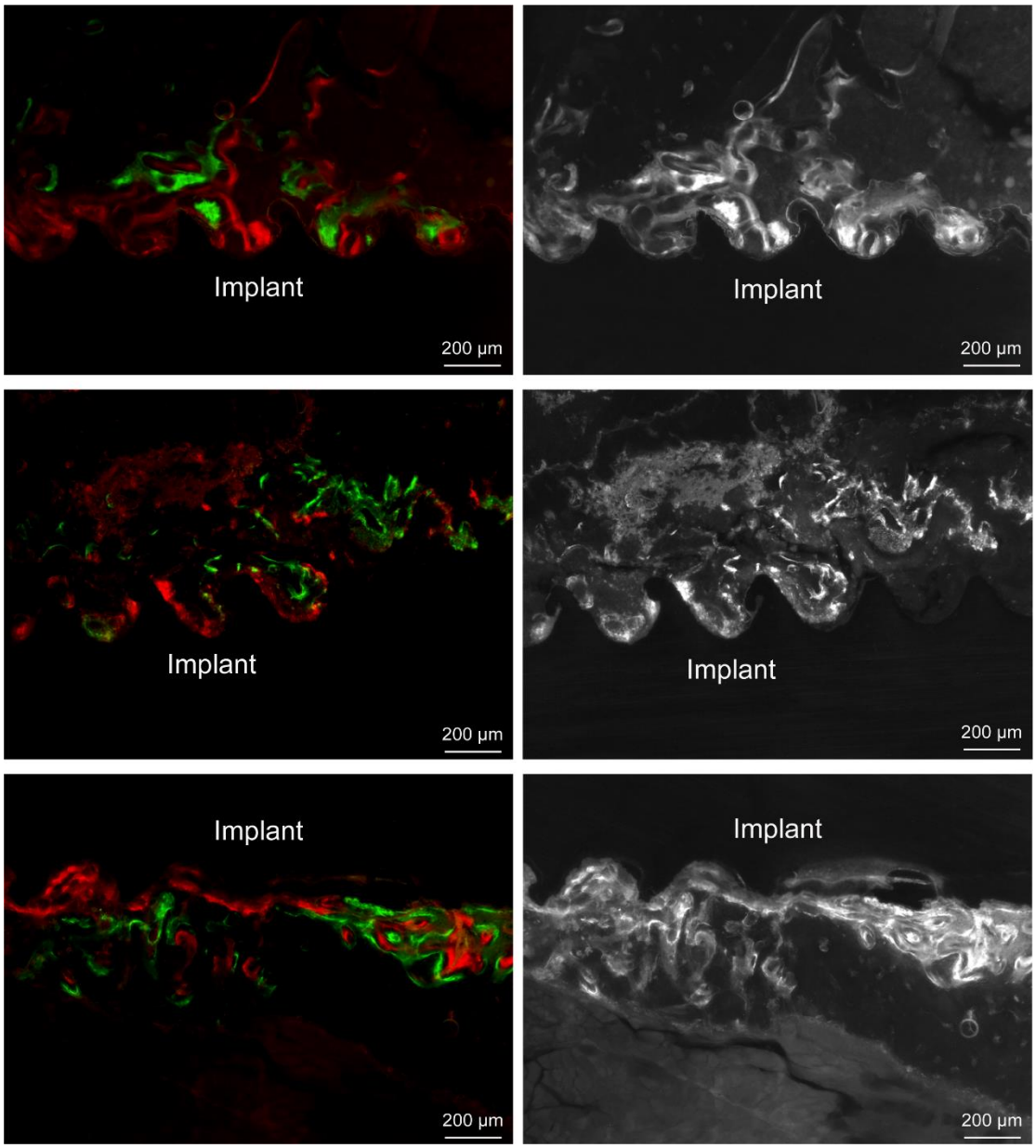

Figure S22 Merged two-channel fluorescence images of the Ti group at 1 month shown in color (left) and in black/white (right). The right image is for better presentation of the position of the screw.

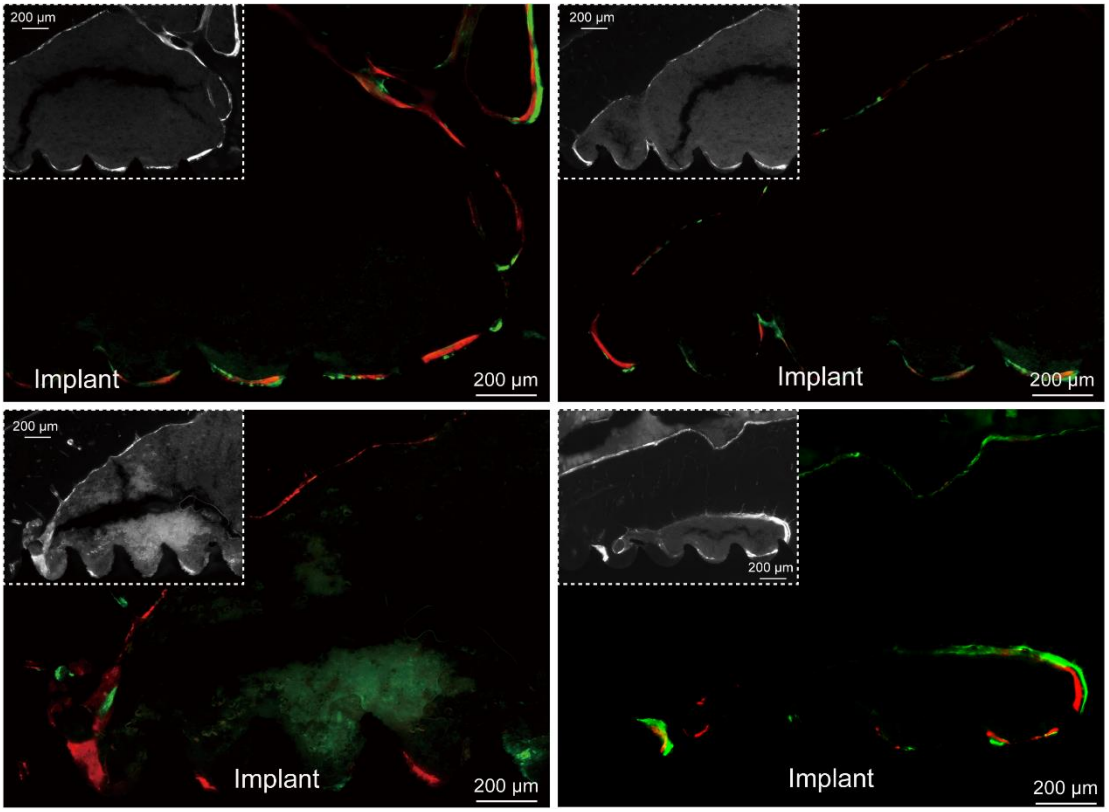

Figure S23 Typical two-channel fluorescence images of the Ti group at 5 months. The insets are the corresponding black/white images to better show the position of the screw.

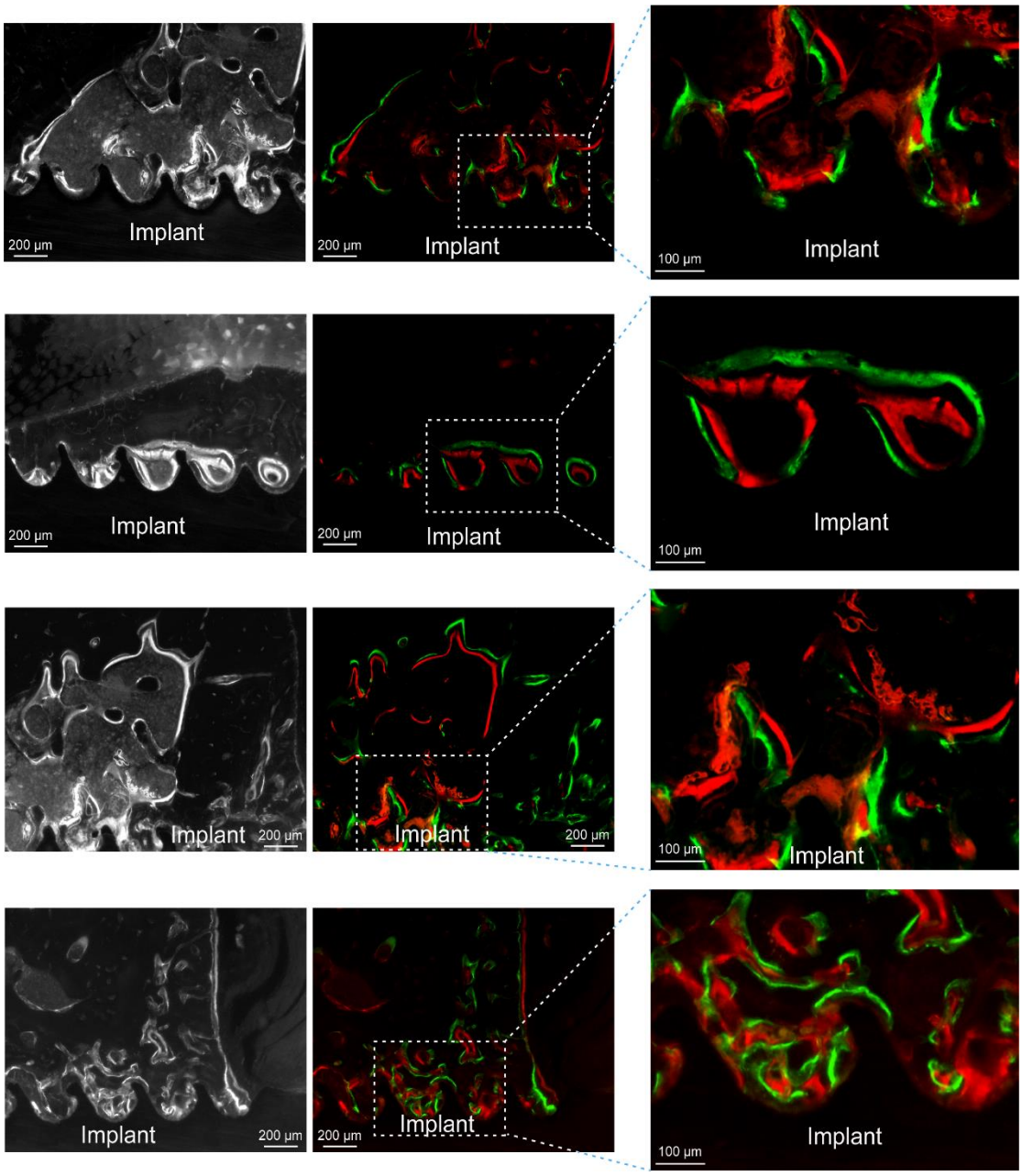

Figure S24 Typical double-labeling immunofluorescence images of the Ti-PDA-Fg group at 1 month.

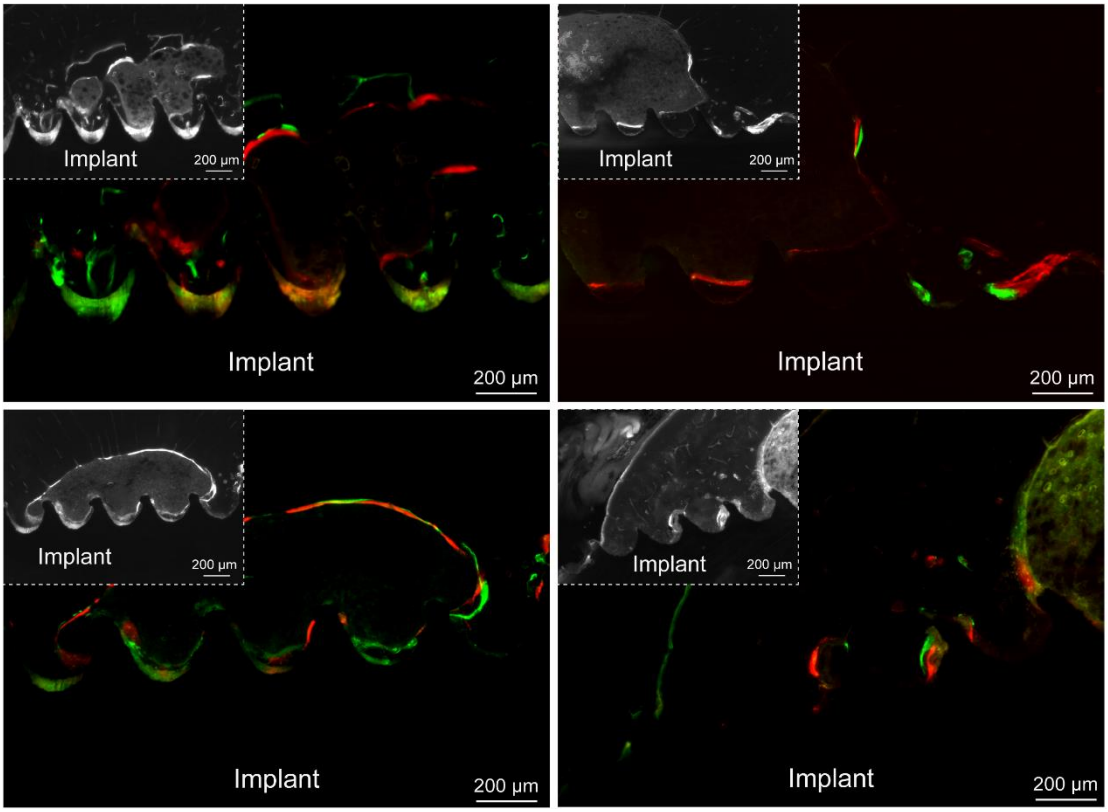

Figure S25 Similar to Fig. S24 except at 5 months.

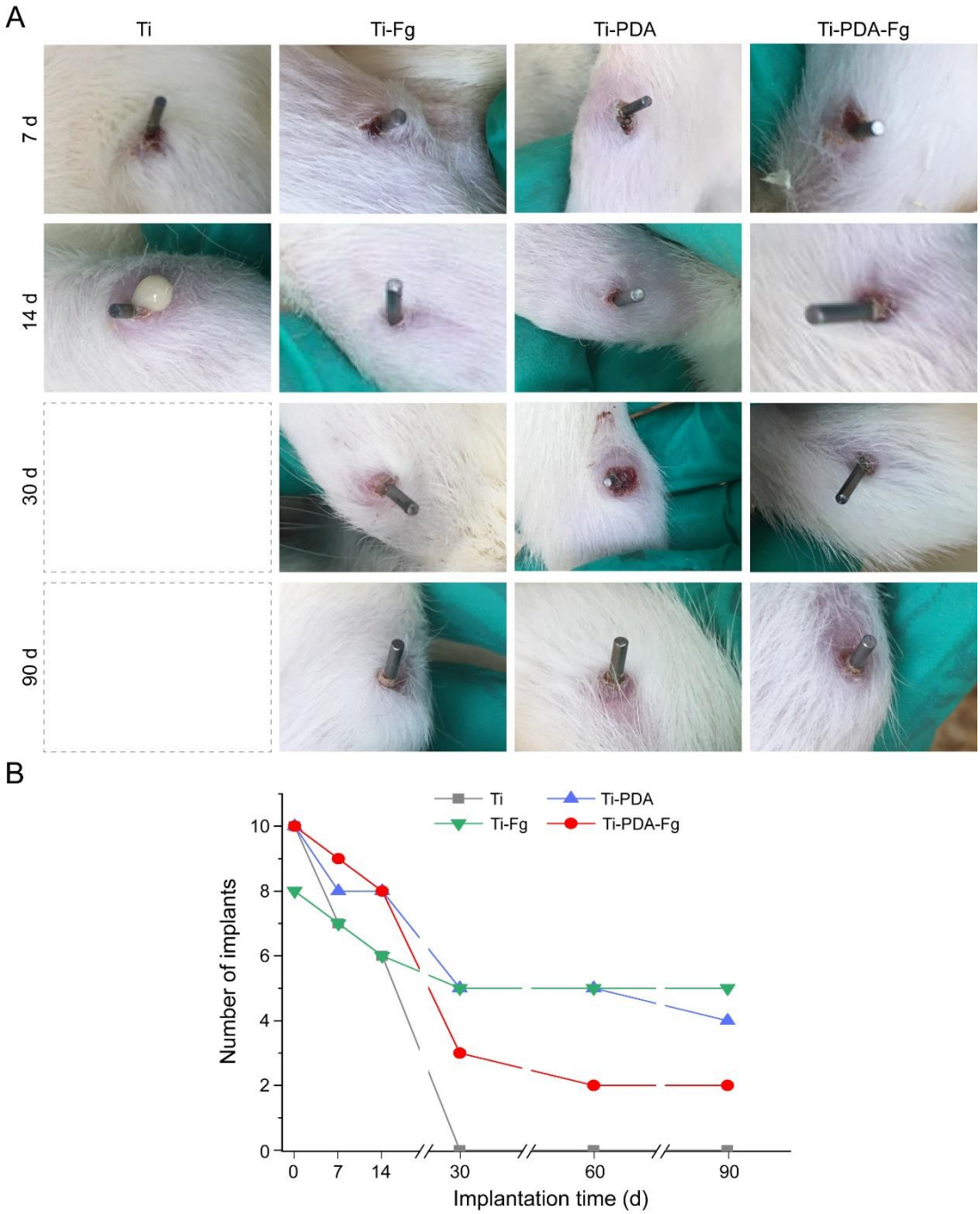

Figure S26 The first round of screw implantation into legs of SD rats. (A) The photograph of implants and wounds at the indicated time points. The lack of images for Ti implant at 30 days and 90 days is owing to that all the implants fall due to infection. (B) The number of the indicated implants as a function of implantation time.

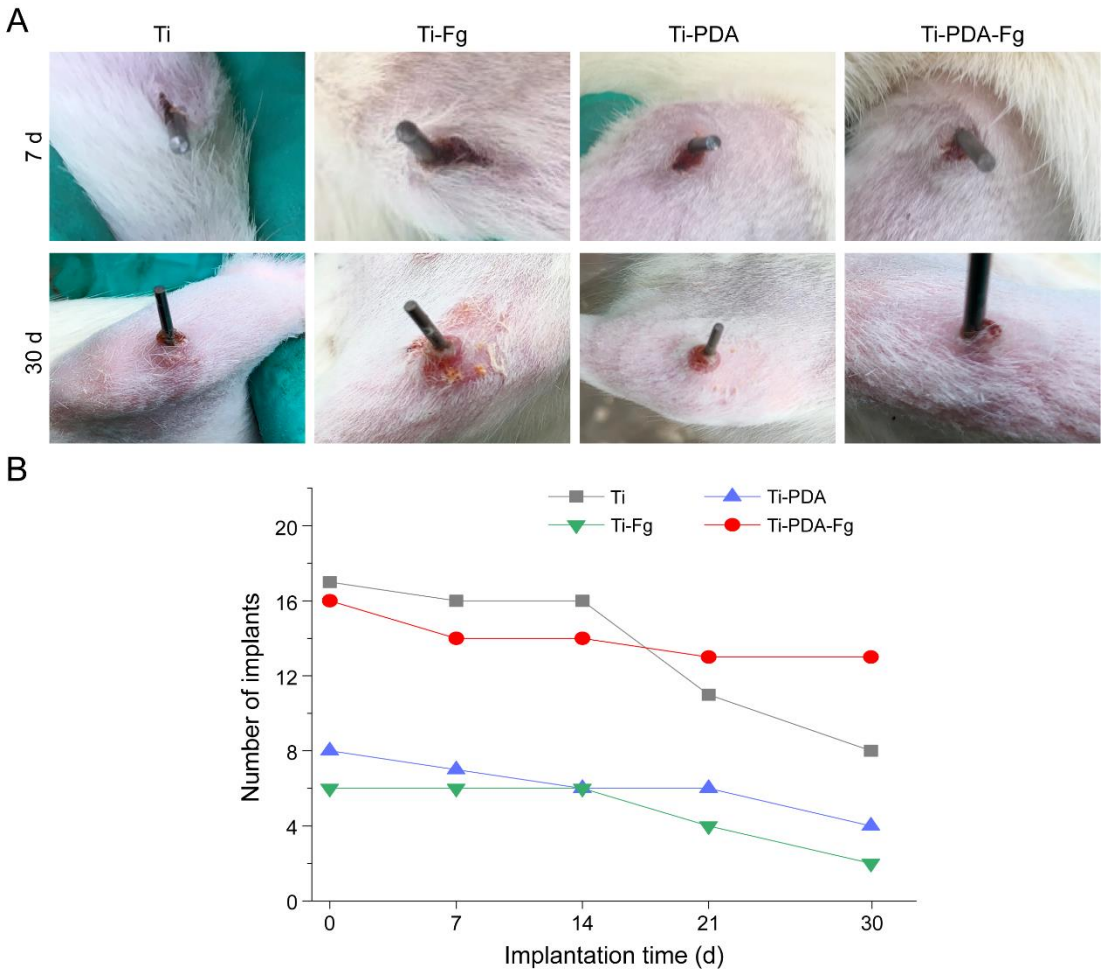

Figure S27 The second round of implantation experiment. (A) The global views of implants and wounds in SD rats. (B) The number of the indicated implants as a function of implantation time.

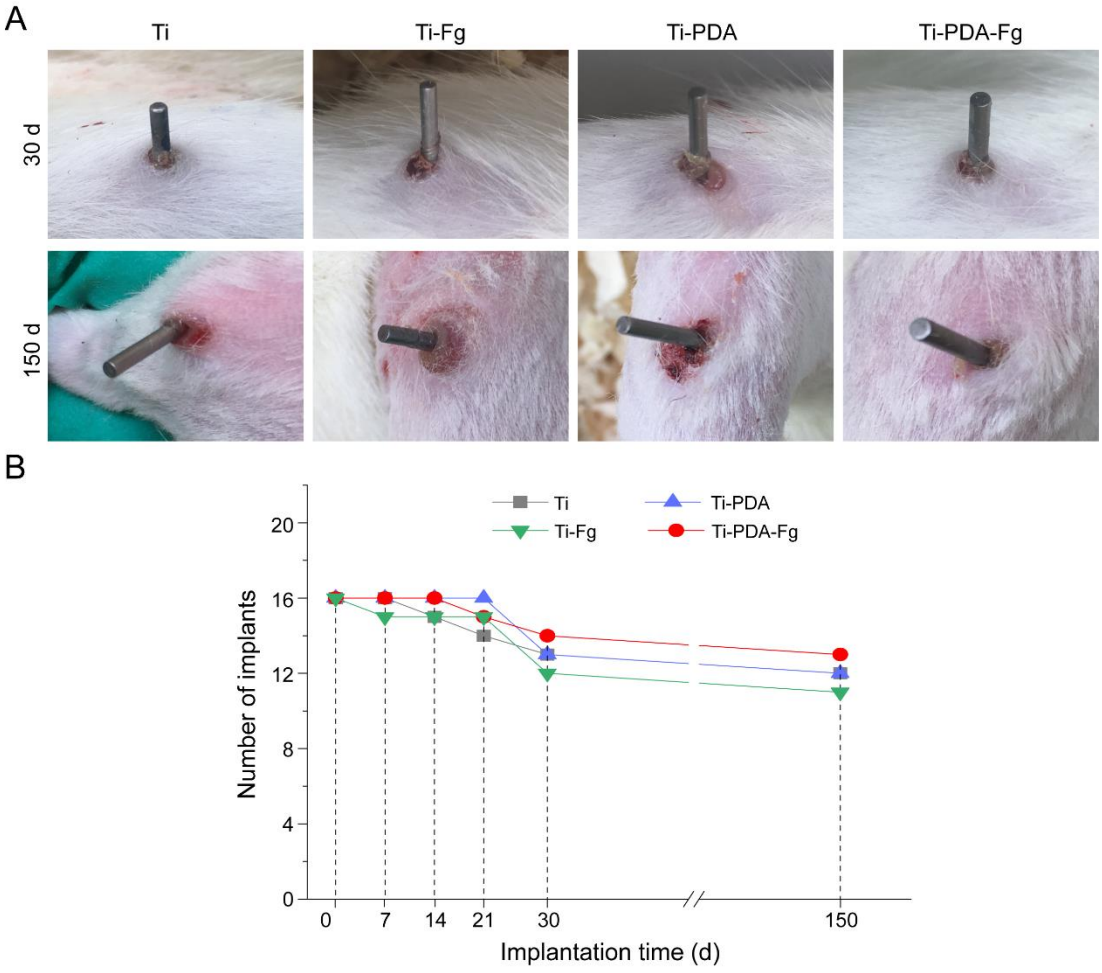

Figure S28 The third round of screw implantation. (A) The photograph of implants and wounds at the indicated time points in SD rats. (B) The number of the indicated implants as a function of implantation time.

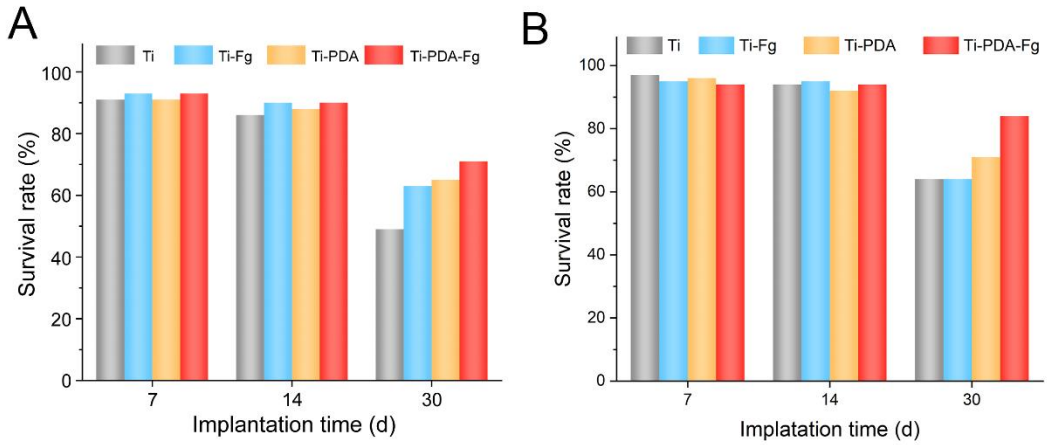

Figure S29 Comprehensive comparison of percutaneous implanting of metal screws with and without surface modification by macromolecules after combining all of data in the three rounds of implantation experiments. (A) The average survival rate of all the three implantation experiments of different samples. Here, the survival rate was calculated by the number of the remaining screws in the legs of the SD rats over that of the initially implanted screws; or the falling rate of the transcutaneous screws is reflected by "100% – survival rate". (B) Similar to (B) except that the statistics were carried out only for the second and the third rounds of implantation.